

A System for Tracking Kinematics of the Human Knee with Sequential MR Image Sets:
Reliability of Coordinate Systems and Accuracy of Motion Tracking Algorithm

Amy L. Lerner*, Jose G. Tamez-Pena†, Jeff R. Houck#, Jiang Yao*, Heather L. Harmon#,
Arthur D. Salo*, Saara M. S. Totterman*^

Departments of Biomedical Engineering*, Radiology^,
and Electrical and Computer Engineering†

University of Rochester

Ithaca College Physical Therapy Program# - Rochester Campus

Corresponding Author: Amy L. Lerner
Asst. Professor
215 Hopeman
Box 270168
Department of Biomedical Engineering
University of Rochester
Rochester, NY 14627-0132

716-275-7847
amlerner@me.rochester.edu
fax: 716-256-2509

Abstract:

The use of magnetic resonance imaging has been proposed by many investigators for establishment of joint reference systems and kinematic tracking of musculoskeletal joints. In this study, the intraobserver and interobserver reliability of a manual digitizing strategy is quantified for seven sets of MR images of the human knee joint. Standard errors of the measurements of tibio-femoral orientations were less than 2.6° , and displacements were less than 1.2 mm. An automated motion tracking algorithm is also validated with a controlled motion experiment in a goat knee joint. The controlled displacements prescribed in our motion tracking validation were highly correlated to those predicted (Pearson's correlation = 0.99, RMS error = 0.25 mm). Finally, the system for anatomic reference system definition and motion tracking is demonstrated with a set of MR images of *in vivo* passive flexion in the human knee.

Keywords: knee joint, kinematics, magnetic resonance imaging, motion tracking

Introduction:

Magnetic resonance (MR) imaging is becoming an increasingly important tool for *in vivo* studies of musculoskeletal biomechanics. It may be used to non-invasively obtain accurate geometric and anatomical information for both normal and injured joints. This information may be coupled with other analysis and modeling tools such as gait analysis and finite element modeling to test many hypotheses regarding joint function and the effect of injuries [1]. In addition, new techniques have been developed to allow motion or loading within the MR scanner, thereby allowing investigation of kinematics or soft tissue deformations [2-4]. Integration of MR imaging with these other tools generally requires either manual or automated image analysis techniques to establish coordinate systems, segment objects or track motion of these objects. However, little is known about the reliability and accuracy of these techniques.

Several recent studies have focused on determining levels of reliability and accuracy associated with using new imaging techniques to track musculoskeletal motion [2, 5]. Piazza *et al* suggested tibiofemoral segment orientation errors of 10° using palpated surface landmarks, confirming a need for methods to more consistently define tibia and femoral coordinate axes [6]. Some previous studies used radiographs to establish segment coordinates

[7], however, no reliability studies have reported the segment orientation errors associated with using fiducial points from MR images. Neu *et al* tested the accuracy of three surface registration algorithms to track carpal bone motion with CT images, but no similar studies evaluate the accuracy using MR images [5]. An MR image based motion tracking algorithm has demonstrated the ability to track shoulder and knee kinematics, however its accuracy has not previously been documented [8].

The purpose of this study was to evaluate the reliability of establishing anatomic reference frames using bony landmarks from MR images, and the effect of inconsistencies on establishing tibiofemoral orientation. In addition, the accuracy of an MR image based motion tracking algorithm is evaluated for quantification of knee motion and demonstrated by tracking *in vivo* passive flexion of the human knee.

Methods

A technique for defining an anatomic coordinate system was developed [9] and evaluated in magnetic resonance image sets from seven human knees. A three-dimensional image-based motion tracking algorithm was investigated and its accuracy evaluated with images of a goat knee. Finally, the coordinate system definition and motion tracking system are demonstrated in an *in vivo* passive flexion of the human knee joint.

Coordinate System Definition and Reliability Evaluation in the Human Knee Joint:

Seven knee image sets from five adult volunteers were analyzed for this study. Subjects had an average age of 32 +/- 8.7 years, average height of 1.7 +/- 0.13 m, and average weight of 68.9 +/- 11.3 kg and gave consent for the procedure. A single knee of three subjects and both knees of two subjects were imaged, generating seven sets of knee images. Subjects were positioned supine with the knee flexed to approximately 10°. For each knee, 3-D gradient recalled echo (GRE) sequences were collected in the sagittal plane, with slice thickness of 1.5 to 1.7 mm. The fields of view were between 15 and 17 cm, yielding in plane resolutions between 0.58 mm/pixel and 0.66 mm/pixel. An isotropic volume was generated and IRIS Explorer software was used to generate axial images with an in plane resolution equivalent to the sagittal slices (IRIS Explorer 2.2.2). Sagittal and axial images were analyzed using NIH image software (National Institutes of Health, USA). Using definitions for nine bony landmarks, (Figure 1) two observers recorded the (x, y, z) coordinates for each landmark two times. For the proximal femur and tibia, mid-diaphyseal points were identified by outlining the diaphysis and determining the centroid of each cross-section. The standard error of the

measurement (SEM) and Pearson correlation coefficients within an observer and between observers were used to judge the consistency of determining landmarks.

Anatomic reference systems were then created for the tibia and femur by creating unit vectors between landmark points and cross-products to define orthogonal systems as follows.

Tibia: The inferior/superior axis is defined using the unit vector from the distal to proximal mid-tibial diaphysis points. This vector is crossed with a vector connecting the medial and lateral tibia points to define an anterior / posterior axis. Finally, the inferior / superior axis is crossed with the anterior / posterior axis to define the medial / lateral axis and guarantee orthogonality. The origin of the tibia coordinate system is then positioned at the medial intercondylar eminence point.

Femur: A unit vector connecting the anterior intercondylar notch and the proximal femur centroid defines the inferior/superior axis. This vector is crossed with a vector connecting the medial and lateral femoral condyle points to define an anterior/posterior axis. The inferior/superior axis is then crossed with the anterior/posterior axis to define an orthogonal medial/lateral axis. The origin of the femur coordinate system is positioned at the intercondylar notch.

Following the method of Grood and Suntay, the relative coordinate system orientations were expressed in the clinical terms of flexion/extension, adduction/abduction, and internal/external rotation [10]. The distance between the two origins was also expressed in the anatomic coordinate systems. The effect of intra- and inter-observer variations in digitizing on the establishment of the coordinate systems were assessed by calculating the Pearson correlation and standard error of measurement (SEM) for each of the three rotations and translations.

Motion Tracking Algorithm:

Analysis of a sequence of kinematic data sets starts with complete segmentation of a single volumetric data set using either automatic or manual segmentation techniques. In this study, an automatic segmentation procedure involving a hierarchical approach of region growing, splitting and merging and statistical relaxation labeling was used [11]. To track motion in subsequent volumes, point correspondences between feature points are predicted using a discrete deformable model formulation. This approach has been shown to be more efficient and accurate than repeated image segmentation [12]. The motion tracking algorithm is based on minimization of the total energy, including the differences in voxel intensity,

gradient magnitude, the Laplacian squared and the mesh deformation energy. For tracking of bones, these segmented structures are treated as rigid bodies and all other tissues are assigned low stiffness properties. A mesh is built connecting randomly selected boundary node points and some interior points of the segmented regions. A gradient minimization algorithm in a multi-resolution framework finds motion between rigid structures, and the optimal mesh configuration defining the nodes' displacements, continuing until all volumes in the series have been segmented. Results of the motion tracking algorithm include definition of translations of the centroids and rotation matrices for the segmented structures relative to the global coordinate system for each image set of the motion series. To test consistency of the algorithm, ten sets of random node points were selected and the tracking procedure repeated.

Validation of Bone Motion Tracking

In this experiment, the tibia and femur of a goat knee joint were mounted in a frame that held the femur fixed while the tibia could be translated medially and anteriorly. The distal tibia pot is held in a plastic block that may be moved along threaded rods and fixed in place with one or more plastic spacers to control the magnitude of displacement (Figure 2). To allow unimpeded joint motion, the ACL, PCL and collateral ligaments were resected. Eight image sets were obtained with variations in tibia position including up to 6 mm out-of-plane translation and 9 mm in-plane translation, and two repeats of the original position. Image sequences were fast 3D GRE images, with a 12 cm FOV, 256 x 256 matrix, and 60 slices of thickness 0.9 mm, providing a spatial resolution equivalent to the human knees, relative to bony dimensions (i.e. one slice = 2% of medial/lateral dimension of bone, one pixel = 1.5% of anterior/posterior dimension). A phased array surface coil was custom designed for placement over the knee joint. Three markers were placed on the frame and their positions monitored within MR images to insure alignment with the MR coordinate frame, and to confirm lack of motion of the frame during translation of the tibia. Image data sets were processed to segment the tibia and femur in the original position, followed by motion tracking to the seven additional positions. Translations of the tibia centroid and orientations of the principal axes relative to the global reference frame were calculated for each test position and compared to the imposed motion. The root mean squared (RMS) difference and Pearson correlation were calculated.

Demonstration of Motion Tracking in *in vivo* Passive Flexion of the Human Knee:

A series of six routine GRE image sequences were collected as a subject flexed his knee approximately 4° between each sequence from full extension to the limits of the MR

scanner. The motion tracking algorithm was used to quantify segment orientation and translation of the tibia and femur for each MR image. Anatomic points were digitized (Figure 1) for the first set of MR images (full knee extension) and assumed to remain at a fixed position relative to each segment. A coordinate transformation was used to predict the position of each anatomic landmark in subsequent MR images throughout knee flexion. The predicted landmark locations were then used to describe tibio-femoral motion in clinical terms of flexion/extension, abduction/adduction, and internal/external rotations, and motions in terms of anterior/posterior, medial/lateral and inferior/superior shifts. The anatomic points predicted by the motion tracking algorithm were then compared to manually digitized points from each set of MR images, and RMS differences were calculated.

Results:

The average SEM for nine digitized points was 0.51 mm for inter-observer, and 0.41 mm for intra-observer differences (Table 1). Maximum SEMs of 3 mm were associated with points establishing medial/lateral axes. In several cases, these differences were smaller than the in-plane resolution, suggesting practical differences of +/- 1 pixel for these landmarks. Correlations for intra-observer and inter-observer identification of each landmark were above 0.95. The effect of these variations on coordinate axis definition resulted in inter-observer SEMs of 1.2, 1.0, and 2.6 degrees for flexion/extension, adduction/abduction, and internal/external rotation (Table 2). Distances between the anatomic origins had inter-observer SEMs of 0.73, 0.65, and 0.34 mm for anterior/posterior, medial/lateral, and inferior/superior directions.

The motion tracking algorithm confirmed the fixed position of the goat femur in the validation experiment. This algorithm predicts motion in discrete steps equivalent to one-third of a pixel or one-third of the slice thickness. In the tibia, the estimated translation of the centroid was highly correlated to the imposed motion, with a Pearson correlation of 0.99, and an RMS error of 0.25 mm. Slight systematic underestimation of translations was identified, indicated by a regression slope of 0.93. No rotations of the tibia or femur were imposed in the validation experiment, as confirmed by estimated rotations averaging 0.19° , and less than 1° for both bones. The effect of these small rotations was evaluated by multiplying each rotation matrix by unit vectors in the principal directions. The predicted motion was then scaled by 25 mm, approximately the radius of the goat femur and tibia. The average rotation induced error in motion of a point on the periphery of the goat femur or tibia is 0.001 ± 0.16 mm. The

maximum rotation induced error was 0.41 mm, which is approximately equal to one-third of the slice thickness of the image set. Repeated selection of random points for motion tracking yielded standard deviations for translations of the tibia averaging 0.07 mm.

Using the anatomic reference system and the motion tracking algorithm, the subject's passive knee flexion reached 19°, and was associated with an internal rotation of 0.5°, and abduction of 1.7°. In addition, the relative displacements included a posterior drawer of 3 mm, medial shift of 1.4 mm, and joint distraction of 6 mm. Comparison of the manually digitized points to predicted points confirms a close match for flexion patterns (Figure 3), but poorer matches for other rotations and translations. Average RMS difference between digitized points and the location of the points as predicted by the motion tracking algorithm was 1.71 mm (Table 4). The RMS errors averaged 1.9° for rotations and 2.3 mm for translations, with Pearson correlations above 0.95 only for flexion and inferior/superior translation.

Discussion

Our study investigated the use of MR imaging to both establish anatomic coordinate systems and to track musculoskeletal kinematics of the human knee joint. The assessment of the accuracy, reliability and repeatability of these methods allows us to consider the practical limitations of each technique for use to quantify kinematics alone and in conjunction with other techniques such as finite element modeling and gait analysis.

Our investigation demonstrated good reliability within and between observers in the consistent identification of bony landmarks from MR images to define anatomic coordinate systems. Piazza *et al* [6] suggested errors as high as 13° in locating the medial/lateral axis using palpated surface landmarks. With the MR images, this axis was also most susceptible to errors, however, our maximum difference detected was a 6.9° shift in the orientation of the axes, and on average the error is much smaller (0.8° intraobserver, and 2.6 interobserver). This finding suggests that the use of MR images results in smaller differences in orientation compared to palpated surface landmarks. Studies [6, 13] have shown that small errors in locating segment axes are propagated into knee kinematics, making comparisons across subjects more difficult. This is especially true in the transverse and frontal planes of the knee when the overall magnitude of motion is small during activities such as walking. Hence, these points from MR images, some of which are similar to a previous study [2], provide an

alternative to establish segment axes of the tibia and femur that potentially increases the consistency of kinematic recordings for comparisons across subjects.

Findings of this study suggest that the use of MR images to locate axis systems can be a useful research method if proper techniques are followed, and selected points are carefully defined. Our points were selected after trial of several options for each axis [9]. Selection of points using multiple image sets (i.e. axial and sagittal images) improved the reliability for both intra and interobserver variations. For example, the inferior /superior location of the proximal tibia points were established in a sagittal image set, then medial/lateral locations are digitized from axial images. In addition, it is important to note that inconsistencies in establishing specific digitized points do not always result in errors in the orientation of the axis. This was particularly true with digitizing the medial/lateral axes of the bones, the consistency of which appears to be better than using external bony landmarks. Further use clinically may depend on further refinement of anatomic points, cost, time, and availability of technology. Once trained, our digitizers could complete one image set in approximately thirty minutes, including time to prepare the axial set of images from the collected sagittal images.

The errors identified in digitizing landmark points, while sufficient for establishing anatomic reference systems, suggest that this method may not be adequate for tracking of complex motions, or for applications requiring greater accuracy such as finite element modeling. For example, errors of 1 mm could predict an unrealistic 50% deformation of a 2 mm thick cartilage layer. The motion tracking algorithm provides excellent tracking ability (RMS error = ± 0.25 mm, $< 1^\circ$ rotation) for tibiofemoral relative motion comparable in magnitude to that expected in an ACL deficient knee. Our validation used a goat knee for convenience, with spatial resolution carefully matched to the human knee images. Although there are minor differences in signal to noise ratios and anatomic feature characteristics between the goat and human knee images, these differences are not expected to have a significant impact on the validity of motion tracking in the human knee. Because the spatial resolution of the goat images are matched to the human, the magnitude of the RMS error in the goat knee likely reflects a potential error of ± 0.37 mm for motions of up to 12 mm. The systematic nature of the error implies that errors will be smaller for the typically smaller motions.

These errors are comparable, or smaller than those detected by Neu *et al* in their study of wrist kinematics using CT image surface registration techniques [5]. While our approach used both surface and interior feature points for registration, it could be similarly challenged

by the small, complex bones in the wrist. Techniques such as roentgen stereophotogrammetric methods [14] have exhibited much smaller errors, however they require implantation of beads or other markers, thereby limiting their applicability in clinical research. Magnetic resonance imaging is non-invasive and requires no radiation exposure, therefore offering more convenience for repeated trials or longer imaging sequences. Although the MR scanner can introduce limitations in subject positioning or the amount of motion feasible, several investigators including ourselves, are exploring methods to apply loading or introduce motion within the confines of the clinical scanner [3, 4, 15]. This motion tracking technique may also be useful in imaging studies of experimental animals in which scanner size limitations are less significant [16].

Our demonstration of the motion tracking algorithm in passive flexion of the human knee identifies the expected pattern of motion, including both flexion and the associated displacements and other rotations. As anticipated, a small degree of internal rotation and abduction are predicted by the motion tracking during the nearly 20° of knee flexion. Although correlations between the predicted and digitized knee flexion are strong ($r^2 > 0.9$), the abduction and internal rotation are poorly correlated ($r^2 < 0.2$) (Table 3). Variations between the digitized and predicted points in the proximal tibia and distal femur are responsible for this lack of correlation. As the knee is flexed, identification of the proximal tibia points is highly inconsistent, since they do not represent true anatomic landmarks (Table 4). The point representing the distal femur is one of the few points whose medial/lateral location is dependent on the selection of a sagittal slice, rather than a point from an axial image. Therefore, the slice thickness of 1.5 mm causes a larger discrete error than the in-plane resolution of 0.47 mm/pixel. This use of a slice location is also critical in causing a lower correlation between predicted and digitized medial tibial displacement. Therefore, although selection of these points was sufficiently accurate to consistently establish an initial reference coordinate system, the digitizing may be inadequate for tracking of motion.

In addition to providing greater accuracy for motion tracking than manual digitizing, the algorithm also allows more rapid processing. This algorithm currently requires approximately 30 minutes for the initial segmentation procedure, followed by two to four minutes for each subsequent image set. This processing is unsupervised and requires minimal user input. Our current platform is a Pentium III computer (800 MHz) running a Windows 2000 operating system. To express the motion tracking results in clinical terms also requires the initial digitizing of points to establish the anatomic reference system and entry into a

spreadsheet to process the motion in subsequent steps. Thus the entire procedure for motion tracking 6 steps requires less than one hour of operator time, and only slightly more computational time.

In conclusion, this study presents a technique for establishment of anatomic reference systems for the knee based on digitizing MR images and evaluates the intra- and interobserver variability of these definitions. This information provides a basis for considering the limitations and practicality of this approach for combination with gait analysis or finite element modeling. While this technique offers improvements over manual palpation of anatomic landmarks, it may still be insufficient for all motion tracking applications. An automated motion tracking algorithm is also validated and demonstrated in passive flexion of the human knee. This system provides an accuracy of ± 0.25 mm for an image set of 0.9 mm slice thickness and 0.47 mm/voxel in-plane resolution, suggesting a potential accuracy in the human knee of less than one-third of the slice thickness. Although the MR scanner presents some practical limitations, this technique offers considerable potential for non-invasive study of joint kinematics.

References:

1. Andriacchi, T.P. and E.J. Alexander, *Studies of human locomotion: past, present and future*. J Biomech, 2000. **33**(10): p. 1217-24.
2. Sheehan, F.T., F.E. Zajac, and J.E. Drace, *In vivo tracking of the human patella using cine phase contrast magnetic resonance imaging*. J Biomech Eng, 1999. **121**(6): p. 650-6.
3. Totterman, S.M.S., Boyd, K.C., Houck, J., Kwok, W.E., Salo, A.D., Lerner, A.L. *MR Imaging of the loaded normal and ACL deficient knee Joint*. in *ISMRM & ESMRMB Joint Annual Meeting*. 2001. Glasgow, Scotland.
4. Vedi, V., A. Williams, S.J. Tennant, E. Spouse, D.M. Hunt, and W.M. Gedroyc, *Meniscal movement. An in-vivo study using dynamic MRI*. J Bone Joint Surg Br, 1999. **81**(1): p. 37-41.
5. Neu, C.P., R.D. McGovern, and J.J. Crisco, *Kinematic accuracy of three surface registration methods in a three-dimensional wrist bone study*. J Biomech Eng, 2000. **122**(5): p. 528-33.
6. Piazza, S.J. and P.R. Cavanagh, *Measurement of the screw-home motion of the knee is sensitive to errors in axis alignment*. J Biomech, 2000. **33**(8): p. 1029-34.

7. Lafortune, M.A., P.R. Cavanagh, H.J.d. Sommer, and A. Kalenak, *Three-dimensional kinematics of the human knee during walking*. J Biomech, 1992. **25**(4): p. 347-57.
8. Tamez-Pena, J.G., S.M.S. Totterman, and K.J. Parker. *Kinematic analysis of musculoskeletal structures via volumetric MRI and unsupervised segmentation*. in *SPIE Medical Imaging '99, Physiology and Fusion from Multidimensional Medical Images*. 1999.
9. Bergeron, K., M. Huson, B. Keisling, L. Mazer, K. Boyd, and J. Houck. *Reliability of Digitizing Anatomical Points from Knee MR Images for Establishing Reference Frames*. in *25th Annual Meeting of the American Society of Biomechanics*. 2001. San Diego, CA.
10. Grood, E.S. and W.J. Suntay, *A joint coordinate system for the clinical description of three- dimensional motions: application to the knee*. J Biomech Eng, 1983. **105**(2): p. 136-44.
11. Tamez-Pena, J., K. Parker, and S. Totterman, *Automatic Statistical Segmentation of Medical Volumetric Images*. Computer Vision and Pattern Recognition, 1998.
12. Tamez-Pena, J., S. Totterman, and K. Parker. *The integration of automatic segmentation and motion tracking for 4D reconstruction and visualization of musculoskeletal structure*. in *IEEE Workshop on Biomedical Image Analysis*. 1998. Santa Barbara CA.
13. Ramakrishnan, H.K. and M.P. Kadaba, *On the estimation of joint kinematics during gait*. J Biomech, 1991. **24**(10): p. 969-77.
14. Selvik, G., *Roentgen stereophotogrammetry. A method for the study of the kinematics of the skeletal system*. Acta Orthop Scand Suppl, 1989. **232**: p. 1-51.
15. Sheehan, F.T., F.E. Zajac, and J.E. Drace, *Using cine phase contrast magnetic resonance imaging to non-invasively study in vivo knee dynamics*. J Biomech, 1998. **31**(1): p. 21-6.
16. Thut, D., Lerner AL, Rubin, SJ, Kwok, WE, Puzas, JE, Seo, GS, Totterman SMS. *MRI for evaluation of early osteoarthritis in the rabbit knee*. in *47th Annual meeting, Orthopaedic Research Society*. 2001. San Francisco, CA.

Acknowledgements: The authors would like to thank K. Boyd, K Bergeron, M. Huson, B. Keisling, and L. Mazer for their efforts related to this work. Financial support was provided by the Department of Radiology of the University of Rochester Medical Center and VirtualScopics, L.L.C..

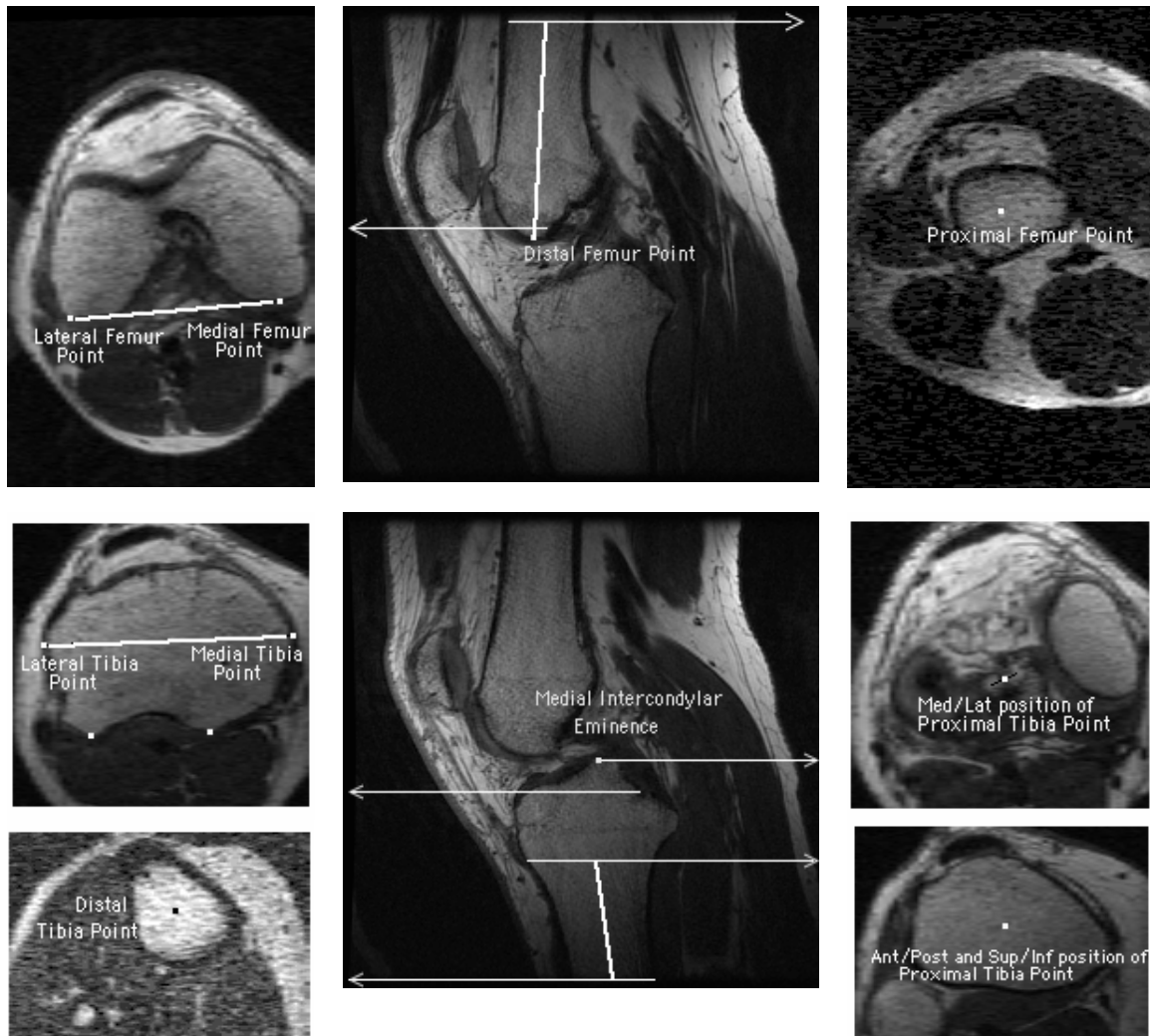


Figure 1. Selection of points for establishment of tibia and femur anatomic reference systems. Tibia origin is placed at the medial intercondylar eminence (MIE), and femur origin at the anterior intercondylar notch. Distal tibia and proximal femur points are located at the centroid of bone cross-sections. Proximal tibia point is located in the medial/lateral direction at the midpoint between the medial and lateral intercondylar eminence. The anterior/posterior location is at the centroid of the tibia cross-section located at the base of the tibia/fibula interface. Medial and lateral tibia points are defined at the tip of the fibular head, creating a line parallel to the most posterior points on the tibia. Medial and lateral femur points are defined at the intercondylar notch based on the most posterior points on the condyles.

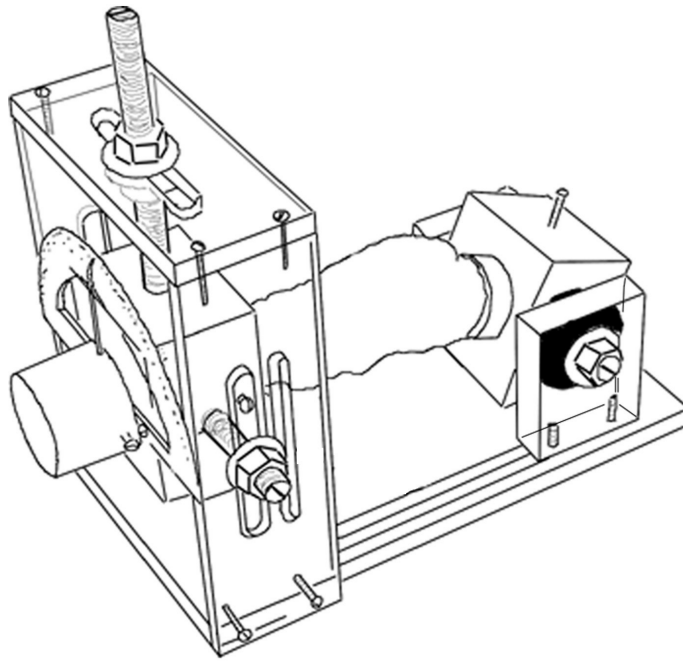


Figure 2: MR-compatible apparatus designed for validation of tibia motion in knee joint. Bones were cut at mid-shaft and potted in PMMA for mounting in the frame. The tibia may be moved in medial / lateral or anterior / posterior directions as well as internal / external rotation. All motions occur in global reference frame. Prescribed motions are then compared to those derived from automatic segmentation and motion tracking algorithms. The frame was placed in a biosafe chamber within the MR scanner with a custom-designed dual-phased array coil positioned over the knee joint (not shown).

Table 1: Intra- and Inter-observer variations in selection of digitized points used to establish anatomic reference frames in tibia and femur. All comparisons resulted in Pearson's correlations >0.95.

		Intraobserver 1			Intraobserver 2			Interobserver		
		M/L	A/P	I/S	M/L	A/P	I/S	M/L	A/P	I/S
Lateral Tibia	SEM	0.77	1.02	0.00	2.88	1.19	0.16	3.04	1.63	0.15
Medial Tibia	SEM	0.91	1.54	0.00	0.77	1.61	0.16	0.81	0.83	0.15
Lateral Femur	SEM	0.89	0.41	0.18	0.63	0.17	0.00	0.94	0.25	0.00
Medial Femur	SEM	0.40	0.11	0.18	0.33	0.17	0.00	1.86	0.61	0.00
Distal Tibia	SEM	0.40	0.17	0.00	0.20	0.29	0.00	0.23	0.19	0.00
Proximal Tibia	SEM	0.43	0.40	0.43	0.37	0.30	0.61	0.41	0.37	0.29
Proximal Femur	SEM	0.16	0.14	0.00	0.35	0.37	0.17	0.18	0.23	0.16
Distal Femur	SEM	0.65	0.22	0.20	0.83	0.58	0.20	0.62	1.06	0.20
Intercondylar Eminence	SEM	0.00	0.20	0.25	0.45	0.23	0.17	0.00	0.27	0.29

Table 2. Variations in calculations of clinical rotations and translations based on intra- and interobserver difference in digitized points. Data include the standard error of the measurement, Pearson's correlation and maximum differences detected.

Clinical Terms - Intra and Interobserver comparisons					
		Intraobserver 1	Intraobserver 2	Interobserver 2	Maximum difference
Flexion / Extension (degrees)	SEM	1.288	1.046	1.213	5.45
	Corr.	0.953	0.970	0.960	
Adduction / Abduction (degrees)	SEM	1.312	0.763	1.008	4.01
	Corr.	0.967	0.982	0.982	
Internal / External (degrees)	SEM	0.805	0.493	2.631	6.88
	Corr.	0.979	0.995	0.880	
Medial / Lateral (mm)	SEM	1.045	1.176	0.654	2.29
	Corr.	0.813	0.730	0.823	
Anterior / Posterior (mm)	SEM	0.604	0.403	0.730	1.49
	Corr.	0.955	0.975	0.908	
Inferior / Superior (mm)	SEM	0.469	0.514	0.340	2.81
	Corr.	0.975	0.976	0.988	

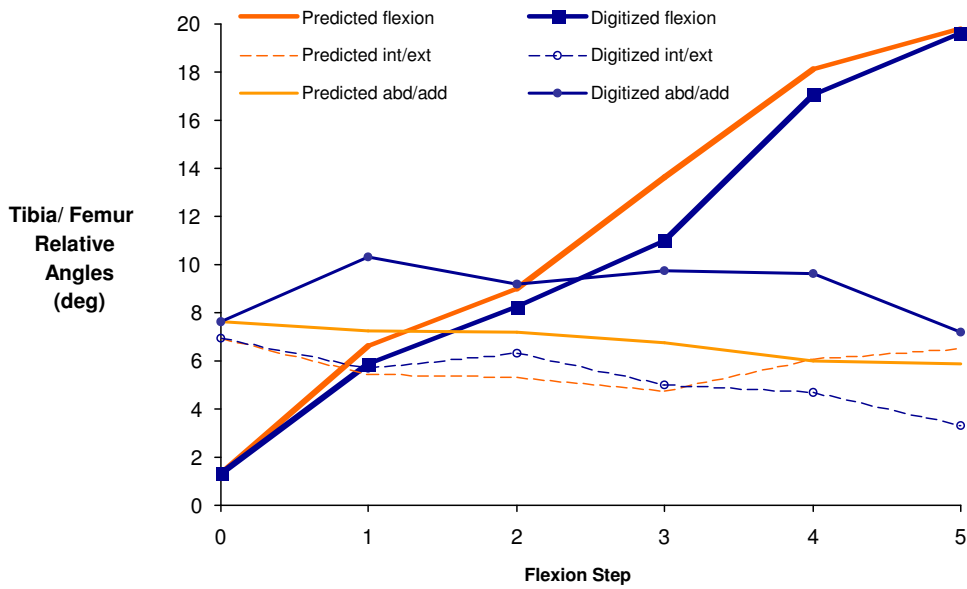
Table 3. Analysis of anatomic position of tibia relative to femur during five steps of passive flexion. Motion predicted by the motion tracking algorithm is compared to anatomic position defined by repeated digitizing of MR images. Data include standard error of the measurement, Pearson's correlation and root-mean squared error.

	SEM Corr.	RMS
Flexion / Extension (degrees)	0.645	1.35
	0.992	
Adduction / Abduction (degrees)	0.644	2.72
	0.147	
Internal / External (degrees)	0.810	1.62
	-0.002	
Medial / Lateral (mm)	0.776	3.00
	-0.866	
Anterior / Posterior (mm)	0.348	2.92
	0.891	
Inferior / Superior (mm)	0.297	0.86
	0.984	

Table 4 Comparison between digitized landmarks and position of landmarks predicted by motion tracking algorithm for passive flexion of up to 19°.

RMS Differences (mm):	M/L	A/P	I/S
Tibia			
Medial Tibia Plateau	1.71	3.96	7.09
Lateral Tibia Plateau	1.87	2.50	5.43
Distal Tibia	0.30	0.69	1.29
Proximal Tibia	1.05	0.75	5.21
Intercond Eminence	0.60	1.31	0.71
Femur			
Distal femur	2.63	1.52	0.16
Proximal femur	0.54	0.21	1.88
Medial condyle	1.03	0.23	0.30
Lateral condyle	1.72	0.63	0.92

Tibia / Femur Relative Angles



Tibia / Femur Relative Displacements

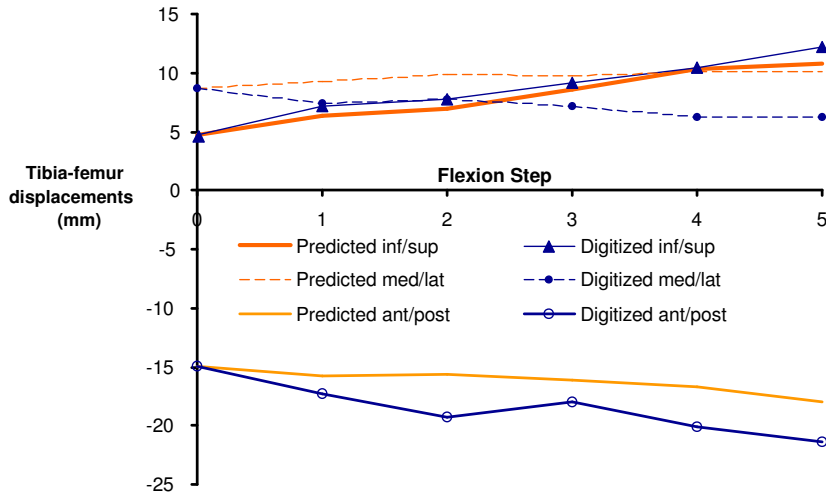


Figure 4: Rotations and translations of the knee joint during passive knee flexion as predicted by the motion tracking algorithm and by manually digitized points.